

Structural Dislocations in Anthracite

Yanqiu Sun,[†] Lawrence B. Alemany,[†] W. E. Billups,^{*,†} Jianxin Lu,[‡] and Boris I. Yakobson^{*,‡}

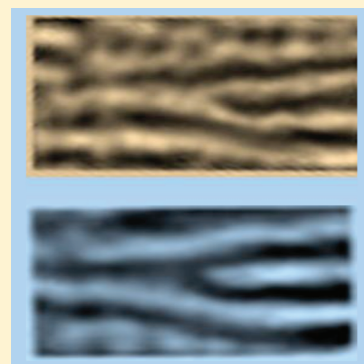
[†]Department of Chemistry, Rice University, Houston, Texas 77005, United States

[‡]Department of Mechanical Engineering and Materials Science and Department of Chemistry, Rice University, Houston, Texas 77005, United States

S Supporting Information

ABSTRACT: Anthracite is composed primarily of polycyclic aromatic hydrocarbons that exist as curved layers of graphenic sheets of various sizes. The bright field high-resolution transmission electron microscopy (HRTEM) image of raw anthracite reveals four kinds of edge dislocations, suggesting that radical-induced dislocation networks are formed during the geologic evolution of bituminous coal into anthracite and that they play an important role in the chemistry of this carbon-rich material. The dislocations result in graphenic layers merging into a massive interconnected network and can explain why samples reductively alkylated by solubilizing dodecyl groups fail to exhibit the high solubility in organic solvents of other similarly functionalized nanomaterials.

SECTION: Nanoparticles and Nanostructures



Carbon nanomaterials promise to find many applications in areas that include electronics, photonics, energy, and sensing. Graphene occupies an important position in this emerging area. In view of our interest in the synthesis of soluble carbon nanotubes^{1–7} and graphene,^{8,9} we have investigated routes to other soluble materials that have a high carbon content. Anthracite is of interest in this regard, as it is composed primarily of polycyclic aromatic hydrocarbons that exist as curved layers of graphenic sheets of various sizes.¹⁰ The carbon content can be as high as 98%. Surprisingly, however, a low level of solubility was achieved when the same protocol (reductive alkylation) that was used to solubilize graphite/graphene was applied to anthracite.¹¹

The functionalization reaction was carried out as illustrated in Scheme 1.

The resulting dodecylated anthracite exhibited low solubility in organic solvents, indicating a low level of reductive alkylation. A detailed investigation using NMR spectroscopy showed that the dodecyl groups were attached to the edges of the anthracite.¹¹ This mode of addition is not unexpected since it has been shown that graphite experiences edge functionalization exclusively under the same conditions.^{9,12}

A study was then undertaken to identify the structural features of anthracite that inhibit exfoliation and thus solubility.¹³ Scanning electron microscopy (SEM) can be used to produce images that contain information about the sample's surface topography. The SEM of a sample of raw anthracite reveals clearly why exfoliation has proven to be difficult. The image presented as Figure 1 reveals a structure in which graphenic layers appear to merge.

The "crosslinking" that is evident from the SEM image suggests that some sp³ hybridized carbon has survived during the

geologic process that leads to coalification of the bituminous coal precursor. Indeed, a solid state ¹³C NMR spectrum of anthracite revealed the presence of a very small amount of aliphatic carbon.¹¹ Raman spectroscopy provides a sensitive technique that can be used to correlate chemical composition with optically discernible morphology of carbonaceous material. The Raman spectrum of a solid sample of the anthracite collected using a Renishaw 1000 microraman system equipped with a 785 nm laser source exhibits a strong broad disorder D band at 1301.3 cm⁻¹ with a shoulder at 1188 cm⁻¹.¹⁴ A much weaker G (graphitic) band at 1597 cm⁻¹ reflects the aromatic ring system (Figure 2).

The observation of dislocations in graphite,^{15–17} carbon nanotubes,^{18,19} and other nanomaterials^{20–25} suggested that dislocations might play an important role in altering the physical and chemical properties of anthracite. Indeed, the bright field high-resolution transmission electron microscopy (HRTEM) image of the raw anthracite (Figure 3) provides the direct evidence for the reluctance (at least in part) of anthracite to undergo exfoliation and thus solubilization during the functionalization reactions. The HRTEM image in Figure 3 reveals four kinds of dislocations, suggesting that the formation of these previously unrecognized radical-induced dislocation networks plays an important role in the processes that occur during the geologic evolution of bituminous coal into anthracite.

The two main types of dislocations are edge dislocations and screw dislocations (dislocations found in many materials are

Received: August 22, 2011

Accepted: September 19, 2011

Published: September 19, 2011

Scheme 1. Reductive Alkylation of Anthracite

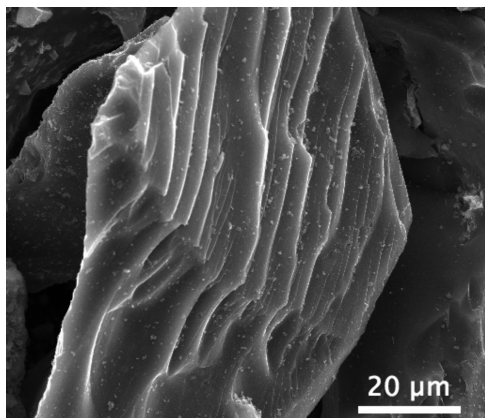
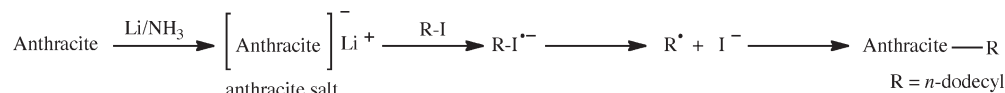


Figure 1. SEM image of anthracite coal from the Mammoth seam in Schuylkill county Pennsylvania.

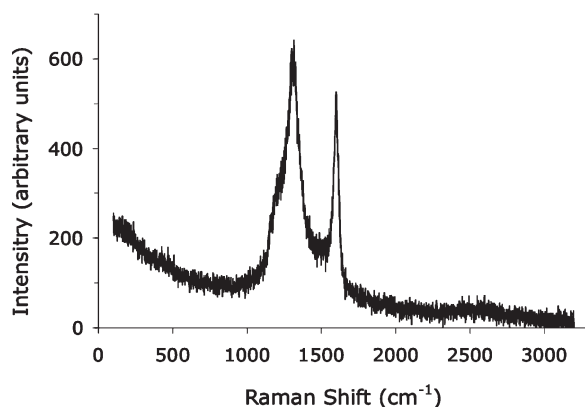


Figure 2. Raman spectrum of anthracite.

mixed, meaning that they have characteristics of both). An edge dislocation is a defect where an extra half-plane of atoms is introduced midway through the crystal, distorting nearby planes of atoms. Figure 3a'' represents the "extra half-plane" concept of an edge type dislocation, with the dislocation line parallel and Burgers vector $|\mathbf{b}| = 3.4 \text{ \AA}$ perpendicular to the basal plane. Important for hindering exfoliation is the transition from the sandwich-type of this dislocation to the somewhat lower in energy ($\sim 0.5 \text{ eV/\AA}$ per our calculations, or about 10% of the dislocation energy) and topologically connected Y-type in Figure 3b,b',b'', where the radical-line of dangling bonds connects to an adjacent plane via change of hybridization to an sp^3 -carbon row (in blue). Solid state ^{13}C NMR analysis of anthracite revealed the presence of a very small amount of quaternary aliphatic carbon¹¹ that would be generated with the formation of the dislocation in Figure 3b'. A screw dislocation (both dislocation line and Burgers vector \mathbf{b} perpendicular to the basal plane, Figure 3c) is even more significant in this respect, as it

essentially renders all planes into one continuous spiraling plane, inseparable without breaking the covalent bonds between the sp^2 -hybridized carbons. It can be visualized as a result of cutting (normal to the basal plane) a crystal part way through, and then slipping along the cut by one lattice parameter and reconnecting the bonds. It comprises a structure in which a helical path is traced around the linear defect (dislocation line) by the atomic planes in the crystal lattice (Figure 3c'').

Both dislocation types can be identified in the sample of anthracite that we have investigated. TEM image simulations of these dislocations (identified as a–d in the TEM image) are shown in Figure 3 as a''–d''. A sandwich-type edge dislocation with a semiplane between two graphene layers is shown as a''. The extra plane in a'' shows the radical atom-sites colored red. The growing graphenic layer in a'' is positioned to react by radical addition to the aromatic rings of a parallel graphenic layer. This gives the Y-type dislocation b' as further depicted in b''. This process forms sp^3 -hybridized centers identified by the blue atoms in b''. The chemistry finds ample precedent in recent studies that demonstrate that the addition of carbon-centered radicals to the aromatic rings of graphene is a facile process.¹¹

A helical structure formed from a left-hand screw dislocation of the graphene layers is illustrated in c' and c''. The colored bonds between sp^2 -hybridized carbons in the spiral highlight the dislocation line. Such structures are likely to form as a natural growth path.¹³ This may also result from a process involving a cascade of radical additions in which each graphene layer adds to an adjacent parallel layer. A common dislocation loop consists of two screw dislocations running in opposite directions (green bonds in Figure 3d'') and connected by the edge-segments (red, in accord with Figure 3a'').

The quaternary aliphatic carbons in Figure 3b'' are the only type of aliphatic carbon directly involved in the dislocations. Solid state ^{13}C NMR also indicated the presence of very small amounts of proton-bearing aliphatic carbons,¹¹ which could easily result from the occasional presence of a CH_3 group on an aromatic ring or the occasional presence of a CH_2 group or perhaps even a $\text{CH}(\text{CH}_3)$ group bridging two aromatic rings. Such bridging would, of course, make exfoliation and solubilization even more difficult.

EXPERIMENTAL METHODS

The anthracite that was used for this study was provided by Dr. John Crelling (Southern Illinois University) and came from the Mammoth seam that is located in Schuylkill county Pennsylvania. The composition of the sample was determined by XPS to be 92% carbon and 6.4% oxygen. Nitrogen, silicon and sulfur were each present in <1%.

HRTEM images are recorded using a JEOL 2100 field emission transmission electron microscope (JEM 2100F TEM) and operated at an accelerating voltage of 200 kV. Raman spectra were collected using a Renishaw 1000 micro-Raman system equipped with a 785 nm laser source. SEM image was recorded

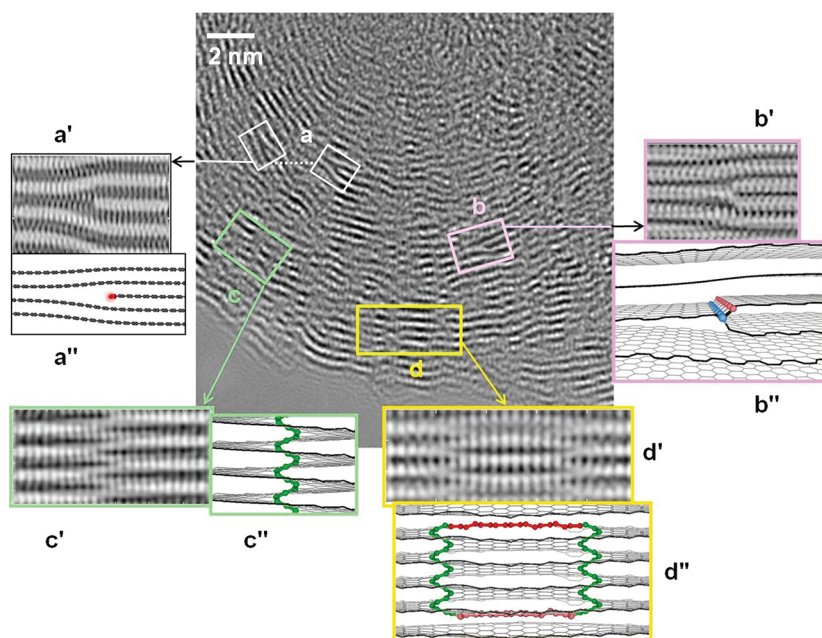


Figure 3. Bright-field HRTEM image of raw anthracite showing four dislocation structures. A radical-rich form of the edge dislocation (a), with simulated TEM (a') obtained from a fully relaxed sandwich atomic structure (a''). Edge-radical sites bind to the adjacent layers resulting into a Y-form (b), containing sp^3 -carbon atoms, marked blue in (b''), and a corresponding TEM simulation (b'). A staggered series of graphene-planes (c) are signatures of screw dislocation helical organization (c''), as its simulated TEM (c') shows. Nearby screw dislocation segments (d) likely belong to the same dislocation loops, completed by the edge segments marked by red edge-atoms (d''), and as its corresponding simulated TEM (d') shows.

using an FEI Quanta 400 scanning electron microscope at an electron beam voltage of 30 kV.

■ ASSOCIATED CONTENT

Supporting Information. Detailed descriptions of the XPS of anthracite. This material is available free of charge via the Internet at <http://pubs.acs.org>.

■ AUTHOR INFORMATION

Corresponding Author

*E-mail: billups@rice.edu (W.E.B.); biy@rice.edu (B.I.Y.).

■ ACKNOWLEDGMENT

This work was supported by the Robert A. Welch Foundation (C-0490 and C-1590), by the Lockheed Martin Corporation (LANCER), and by the National Science Foundation (CMMI, EAGER).

■ REFERENCES

- Liang, F.; Sadana, F. A. K.; Peera, A.; Chattopadhyay, J.; Gu, Z.; Hauge, R. H.; Billups, W. E. A Convenient Route to Functionalized Carbon Nanotubes. *Nano Lett.* **2004**, *4*, 1257–1260.
- Liang, F.; Alemany, L. B.; Beach, J. M.; Billups, W. E. Structure Analyses of Dodecylated Single-Walled Carbon Nanotubes. *J. Am. Chem. Soc.* **2005**, *127*, 13941–13948.
- Chattopadhyay, J.; Cortez, F. J.; Chakraborty, S.; Slater, N. H. K.; Billups, W. E. Synthesis of Water-Soluble PEGylated Single-Walled Carbon Nanotubes. *Chem. Mater.* **2006**, *18*, 5864–5868.
- Moniruzzaman, M.; Chattopadhyay, J.; Billups, W. E.; Winey, K. I. Tuning the Mechanical Properties of SWNT/Nylon 6,10 Composites with Flexible Spacers at the Interface. *Nano Lett.* **2007**, *7*, 1178–1185.
- Ying, Y.; Saini, R. K.; Liang, F.; Sadana, A. K.; Billups, W. E. Functionalization of Carbon Nanotubes by Free Radicals. *Org. Lett.* **2003**, *5*, 1471–1473.
- Ni, C.; Chattopadhyay, J.; Billups, W. E.; Bandaru, P. R. Modification of the Electrical Characteristics of Single Wall Carbon Nanotubes through Selective Functionalization. *Appl. Phys. Lett.* **2008**, *93*, 243113.
- Chattopadhyay, J.; Chakraborty, S.; Mukherjee, A.; Wang, R.; Engel, P. S.; Billups, W. E. SET Mechanism in the Functionalization of Single Walled Carbon Nanotubes. *J. Phys. Chem. C* **2007**, *111*, 17928–17932.
- Chakraborty, S.; Chattopadhyay, J.; Guo, W.; Billups, W. E. Functionalization of Potassium Graphite. *Angew. Chem., Int. Ed.* **2007**, *46*, 4570–4572.
- Mukherjee, A.; Kang, J. H.; Kuznetsov, O.; Sun, Y.; Thaner, R.; Bratt, A. S.; Lomeda, J. R.; Kelly, K. F.; Billups, W. E. Water-Soluble Graphite Nanoplatelets Formed by Oleum Exfoliation of Graphite. *Chem. Mater.* **2011**, *23*, 9–13.
- Aso, H.; Matsuoka, K.; Sharma, A.; Tomita, A. Evaluation of Size of Graphene Sheet in Anthracite by a Temperature-Programmed Oxidation Method. *Energy Fuels* **2004**, *18*, 1309–1314.
- Sun, Y.; Kuznetsov, O.; Alemany, L. B.; Billups, W. E. Reductive Alkylation of Anthracite. Edge Functionalization. *Energy Fuels* **2011**, *25*, 3997–4005.
- Chattopadhyay, J.; Hamilton, C.; Mukherjee, A.; Chakraborty, S.; Guo, W.; Barron, A. R.; Billups, W. E. Graphite Epoxide. *J. Am. Chem. Soc.* **2008**, *130*, 5414–5415.
- Clifford, C. E. B.; Beil, A.; Boland, E.; Grove, L. Exfoliation of Anthracite: Industrially Achievable? *Prepr. Pap.-Am. Chem. Soc., Div. Fuel Chem.* **2004**, *49* (2), 633–635.
- Kudryavtsev, A. B.; Schoff, J. W.; Agresti, D. G.; Wdowiak, T. J. In Situ Laser-Raman Imagery of Precambrian Microscopic Fossils. *Proc. Natl. Acad. Sci. U.S.A.* **2001**, *98*, 823–826.
- Amelinckx, S.; Delavignette, P. Dislocation Loops Due to Quenched-In Point Defects in Graphite. *Phys. Rev. Lett.* **1960**, *5*, 50–52.
- Hennig, G. R. Screw Dislocations in Graphite. *Science* **1965**, *147*, 733–734.

- (17) Hashimoto, A.; Suenaga, K.; Gloter, A.; Urita, K.; Iijima, S. Direct Evidence for Atomic Defects in Graphene Layers. *Nature* **2004**, *430*, 870–873.
- (18) Huang, J.-Y.; Ding, F.; Jiao, K.; Yakobson, B. I. Self-Templated Growth of Carbon–Nanotube Walls at High Temperatures. *Small* **2007**, *10*, 1735–1739.
- (19) Huang, J.-Y.; Ding, F.; Yakobson, B. I. Dislocation Dynamics in Multiwalled Carbon Nanotubes at High Temperatures. *Phys. Rev. Lett.* **2008**, *100*, 035503.
- (20) Wu, Y. Critical Role of Screw Dislocation in the Growth of Co(OH)₂ Nanowires as Intermediates for Co₃O₄ Nanowire Growth. *Chem. Mater.* **2010**, *22*, 5537–5542.
- (21) Bladon, P. B.; Frenkel, D. Free Energy and Structure of Dislocation Cores in Two-Dimensional Crystals. *J. Phys. Chem. B* **2004**, *108*, 6707–6718.
- (22) Song, J.; Bierman, M. J.; Morin, S. A. A New Twist on Nanowire Formation: Screw-Dislocation-Driven Growth of Nanowires and Nanotubes. *J. Phys. Chem. Lett.* **2010**, *1*, 1472–1480.
- (23) Vaz-Domínguez, C.; Aranzabal, A.; Cuesta, A. In Situ STM Observation of Stable Dislocation Networks during the Initial Stages of the Lifting of the Reconstruction on Au(111) Electrodes. *J. Phys. Chem. Lett.* **2010**, *1*, 2059–2062.
- (24) Liu, Y.; Rafailovich, M. H.; Sokolov, J.; Schwarz, S. A.; Bahal, S. Effects of Surface Tension on the Dislocation Structures of Diblock Copolymers. *Macromolecules* **1996**, *29*, 899–906.
- (25) Morin, S. A.; Jin, S. Screw Dislocation-Driven Epitaxial Solution Growth of ZnO Nanowires Seeded by Dislocations in GaN Substrates. *Nano Lett.* **2010**, *10*, 3459–3463.